SYNTHESIS AND TRIBOLOGICAL PROPERTIES OF Nb-DOPED $MoSe_2$ NANOPLATES

XIANGHUA ZHANG[a,b], HUA TANG[c], CHANGSHENG LI[a,c*], SHUAI CHEN[c]
[a]*School of Mechanical Engineering, Jiangsu University, Key Laboratory of Tribology of Jiangsu Province, Zhenjiang 212013, Jiangsu Province, China*
[b]*School of Mechanical Engineering, Jiangsu University of Technology, Changzhou 213001, Jiangsu Province, China*
[c]*School of Materials Science and Engineering, Jiangsu University, Zhenjiang 212013, Jiangsu Province, China*

The Nb-doped $MoSe_2$ nanoplates have been successfully prepared via solid-state thermal (800 ^{o}C) reaction between micro-sized Mo, Nb with Se powders under inert atmosphere in a closed reactor and characterized by X-ray diffractometer (XRD), scanning electron microscopy (SEM). It was found that the morphologies of the as-prepared products changed with the doping of Nb powders. And the sizes of crystallites evidently reduced while the contents of dopant increased within a certain limit (3 wt.%–5 wt.%). The tribological properties of the as-prepared products as additives in paraffin base oil were investigated by UMT-2 multispecimen tribotester. The friction coefficient of the base oil containing Nb-doped $MoSe_2$ nanoplates was lower and more stable than that of $MoSe_2$ nanosheets.

(Received July 19, 2013; Accepted October 27, 2013)

Keywords: nanoplates, Nb-doped $MoSe_2$, solid-sate reaction, tribological properties

1. Introduction

The transition-metal dichalcogenides MX_2 (M = Mo, W, Nb; X = S, Se), which contains an M metal layer sandwiched by two X layers, have been a research area for many theoretical and experimental studies during the last 40 years[1-5]. $MoSe_2$ and $NbSe_2$ are the members of this family. Their structures resemble *a* stacking of sandwiches in each of which a plane of hexagonally arrayed metal atoms lies between two planes of similar arrayed selenium atoms. The bonding within each layer is strong covalent bonding, while the sandwiches are held together by much weaker Van der Waals bonding[6-8]. Due to these weak forces, shearing takes place more easily under high pressure. So the layered molybdenum and niobium dichalcogenides have stimulated considerable interest as lubricants[9-12].

Doping, or alloying nanocrystals provides another fundamental approach to modify the properties of nanocrystals by means of tailoring the crystal's compositions [13]. For example, Hu et al. [14-15] researched the electrical and optical properties of niobium and rhenium doped $MoSe_2$. A. M. Vora [16-19] prepared single crystals of $MoSe_2$ doped with rhenium and indium by direct vapour transport (DVT) technique and found that doping affects the electrical and optical

*Corresponding author: lichangshengujs@yahoo.com

properties of $MoSe_2$ single crystals. T. Joseph Sahaya Anand et al. [20] investigated the synthesis, growth mechanism, optical and semiconducting properties of combinatorial molybdenum sulphoselenide MoS_xSe_{2-x} ($0 \leqslant x \leqslant 2$) thin films. However, there are few reports about the effect of doping on the tribology property of $MoSe_2$.

In this study, Nb-doped $MoSe_2$ nanoplates have been successfully synthesized by a facile solid-state reaction. The SEM images showed the introduction of Nb dopant leaded to an obvious size reduction in addition to the variation in morphologies of the as-prepared products and the Nb-doped $MoSe_2$ nanoparticles exhibited a better friction and wear property than $MoSe_2$ as additives in paraffin base oil.

2. Experimental

2.1 Materials

Elemental selenium, niobium and molybdenum powders were purchased from Shanghai Chemical Reagent Co. Ltd. (Shanghai, China). All chemical reagents were of analytic purity and used directly without further purification.

2.2 Preparation of Nb-doped $MoSe_2$ nanoplate

For the preparation of Nb-doped $MoSe_2$ nanoplates, as a typical case of 5% Nb-doped $MoSe_2$, the mixed powders (molar ratio: Nb:Mo:Se = 5:95:220, an overdose of 20% Se) was energetically ball-milled at 300 rpm (rotation per minute) in the presence of ethanol for 12 h in a planetary ball mill. Then the ball-milled mixture was introduced into 10-ml stainless steel reactor in a nitrogen-filled glove box. The filled reactor was tightly closed with the threaded plug and pushed into the tube furnace. The temperature of the tube furnace was raised to 800 ^{o}C at a rate of 10 ^{o}C/min and the heat was maintained at 800 ^{o}C for 2h. Subsequently the reactor was gradually cooled to room temperature, opened, and the as-prepared powder was obtained. The product was directly characterized without further processing by various analytic techniques.

For comparison, $MoSe_2$, 3% Nb-doped $MoSe_2$ and 10% Nb-doped $MoSe_2$ were also synthesized according to the above process.

2.3 Characterization methods

The X-ray diffraction patterns were recorded using a D8 advance (Bruker-AXS) diffractometer with Cu *Ka* radiation (λ = 0.1546 nm). The morphologies and structures of the samples were characterized by scanning electron microscopy (SEM, JEOL JXA-840A).

Friction tests were performed using a UMT-2 ball-on-disc tribometer (CETR, USA) under lubricated conditions. The as-prepared products modified by dispersing agent sorbitol monooleate (Span-80) was distributed into the paraffin base oil via 60 min ultrasonication, leading to the desired samples with 2 wt.% $Mo_{1-x}Nb_xSe_2$($0 \leqslant x \leqslant 0.1$). The testing of friction reduction and wear resistance was conducted at rotating speed of 50-400 rpm (rotation per minute) and load of 5-40 N for 30 min. The material of upper sample is 40 Cr stainless steel ball with a diameter of 10 mm, hardness of 62 HRC, and the counterpart is 45 steel disc of Φ40 mm×3 mm in size. The friction coefficient was automatically recorded during the contact friction.

3. Results and discussion

3.1 XRD analysis

The XRD patterns of $MoSe_2$ and niobium-doped $MoSe_2$ are illustrated in figure 1. All the reflections have been indexed to the pure hexagonal phase (p63/mmc space group) of $MoSe_2$ with lattice constants a = 3.288 Å and c = 12.90 Å (PDF No. 65-3481). The X-ray diffractogram of $Mo_{1-x}Nb_xSe_2$ in figure 1 clearly show that (002) reflection is of the maximum intensity and thereby indicates the presence of a well-stacked layered structure. The diffractogram for $Mo_{0.97}Nb_{0.03}Se_2$, $Mo_{0.95}Nb_{0.05}Se_2$ and $Mo_{0.9}Nb_{0.1}Se_2$ are similar to those of $MoSe_2$. The refined lattice parameters are listed in Table 1. The lattice parameter 'a' remains constant for all samples while there is a slight amount of increase in 'c' parameter indicates that niobium has been intercalating in between the layers thereby expanding the 'c' parameter. This increase is very small because the amount of niobium incorporated with MoSe2 is also lesser in proportion. As proportion of niobium addition is increased in MoSe2, its X-ray intensity also changed which can be seen from Figure 1. When the proportion is increased to 3 wt.% - 5 wt.%, the intensity is reduced and the widths of the diffraction peaks are broader. The results indicate that the size of particles is decreased. And when the proportion is increased to 10 wt.%, the intensity of the diffraction peaks are increased, which means the size of particles is expanded.

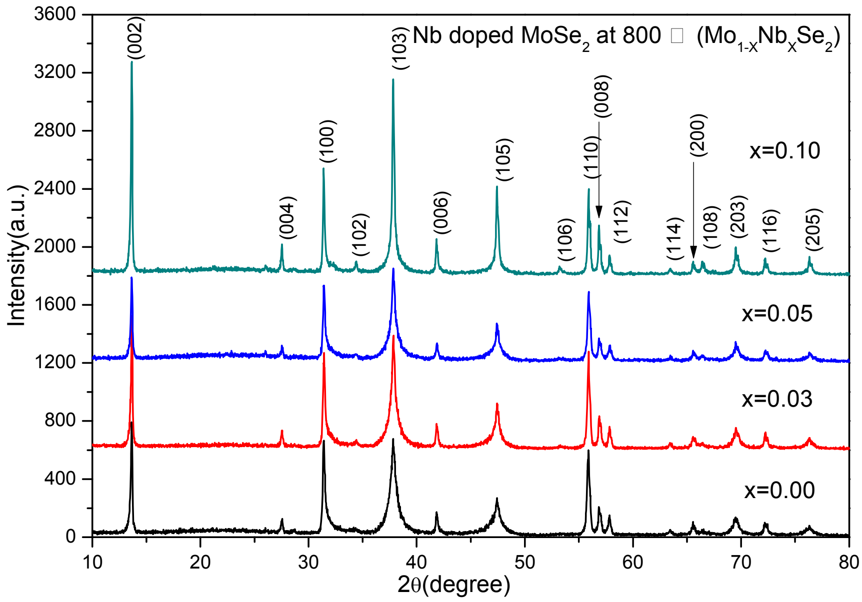

Fig. 1 XRD patterns of Undoped and Nb-doped $MoSe_2$ nanoplates calcined at 800 ^oC

Table 1 Lattice parameters for undoped and Nb-doped $MoSe_2$ crystals.

Material	Parameters		
	a(Å)	c(Å)	c/a
$MoSe_2$	3.287	12.941	3.937
$Mo_{0.97}Nb_{0.03}Se_2$	3.287	12.943	3.938
$Mo_{0.95}Nb_{0.05}Se_2$	3.287	12.946	3.939
$Mo_{0.90}Nb_{0.10}Se_2$	3.287	12.948	3.939
$MoSe_2$(PDF No. 65-3481)	3.288	12.90	3.923

3.2 SEM observations

The morphologies of the $MoSe_2$ and Nb-doped $MoSe_2$ products are primarily investigated by SEM measurement. Fig. 2a shows that the as-prepared pure $MoSe_2$ particles are composed of flakes dominating with diameters of about 1–6 μm and a thickness of about 100 nm. It can be clearly seen that the nanosheets aggregate together. When introduced 3 wt.% Nb powder, the size of the nanosheets is decreased and the nanoflakes became scattered. At the same time, part of nanosheets converted to the hexagonal morphology with the diameter of nearly 500 nm and a thickness of about 50 nm (figure 2b). With the introduction of 5 wt.% Nb powder, the size reduction of the nanosheets is very significant and many sheets have coverted to the hexagonal morphology (figure 2c). And when the niobium addition is increased to 10 wt.% , the as-prepared particles are assemble together and the size is increased(figure 2d). The conclusion is extremely in accordance with the results of XRD analysis.

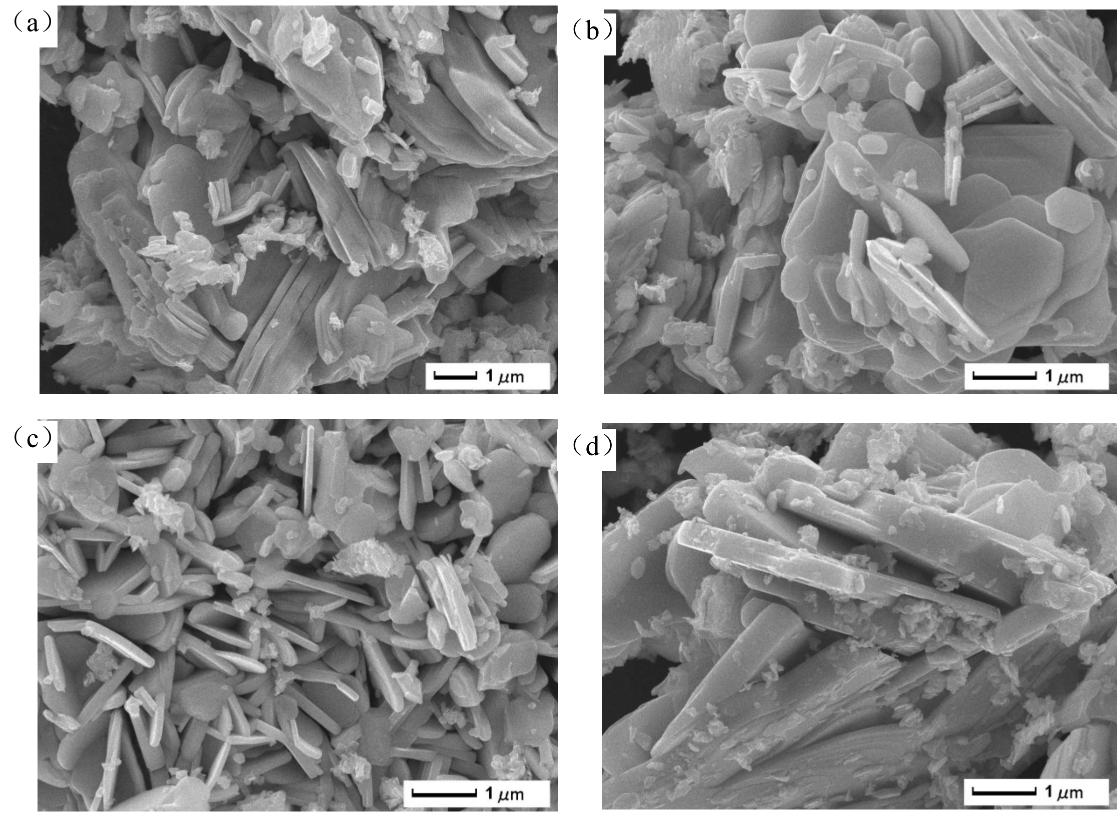

Fig. 2 SEM images of (a) $MoSe_2$, (b) 3 wt.% Nb-doped $MoSe_2$, (c) 5 wt.% Nb-doped $MoSe_2$,

(d) 10 wt.% Nb-doped $MoSe_2$

3.3 Tribological properties analysis

Fig. 3 shows the comparisons of tribological properties among paraffin basic oil without additives and the base oil containing 2 wt.% $MoSe_2$, $Mo_{0.97}Nb_{0.03}Se_2$, $Mo_{0.95}Nb_{0.05}Se_2$ and $Mo_{0.90}Nb_{0.10}Se_2$ at the load of 20 N under diverse speeds. With the rotating speed of 50～400 rpm, the friction coefficient of the base oil containing prepared nanoplates is always lower than that of pure base oil, and it decreases with the dopent percent of the additives no more than 5 wt.%. Especially, the base oil with 2% $Mo_{0.95}Nb_{0.05}Se_2$ nanoplates have lower and more stable friction coefficient compared with other additives.

Fig.4 represents the curve of friction of paraffin basic oil and the base oil containing 2 wt.% additives at the different loads (5 N, 10 N, 20 N, 30 N, 40 N) under a speed of 300 rpm for 30 min. The friction coefficient of base oil without any additive is increased with the load increasing. With the addition of 2.0 wt.% $MoSe_2$ sheets in base oil, the friction coefficient was reduced remarkably when the load is less than 30 N. The friction coefficient of the base oil with 2.0 wt.% $Mo_{0.97}Nb_{0.03}Se_2$ nanoplates is lower than that of the base oil with 2.0 wt.% $MoSe_2$. When the dopent percent of the additives is 5 wt.%, the friction coefficient is lower and stable. But when the dopent percent is increased to 10 wt.%, the friction coefficient is increased with the load increasing. From these results, it can be concluded that the $Mo_{0.95}Nb_{0.05}Se_2$ nanoplates have better anti-wear capability. The $Mo_{0.95}Nb_{0.05}Se_2$ nanoplates with thinner and smaller size will penetrate more easily into the interface with base oil and form thin oil film in the concave of rubbing face, which can decrease shearing stress and bearing high temperature, therefore, exibit a lower friction coefficient.

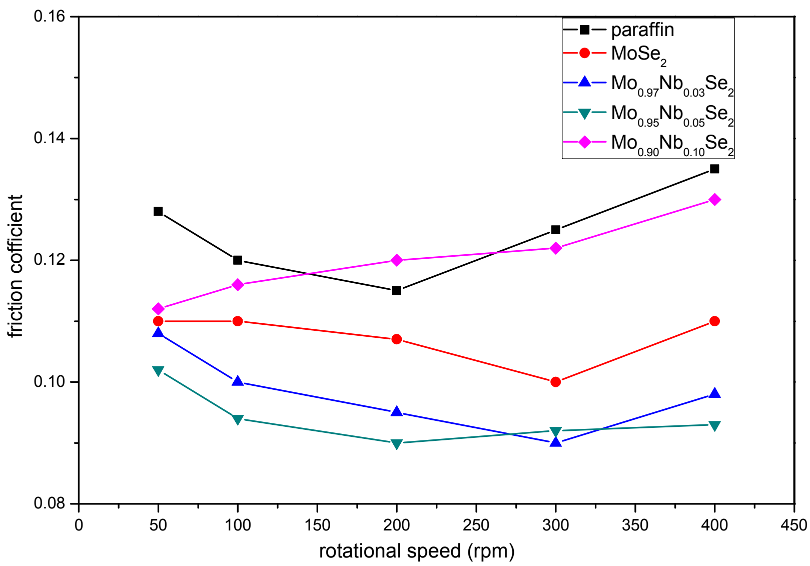

Fig. 3 Variation of friction coefficient as a function of rotating speed for the paraffin base oil and the base oil containing 2 wt.% $MoSe_2$, $Mo_{0.97}Nb_{0.03}Se_2$, $Mo_{0.95}Nb_{0.05}Se_2$ and $Mo_{0.90}Nb_{0.10}Se_2$ nanoplates at the load of 20 N.

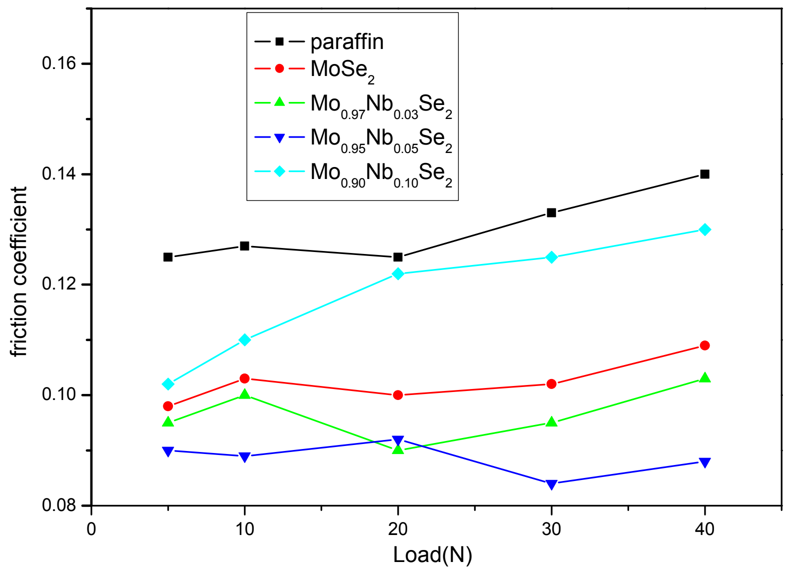

Fig. 4 Variations of friction coefficient of the paraffin base oil and the base oil containing 2 wt.% $MoSe_2$, $Mo_{0.97}Nb_{0.03}Se_2$, $Mo_{0.95}Nb_{0.05}Se_2$ and $Mo_{0.90}Nb_{0.10}Se_2$ nanoplates with increasing load at 300 rpm for 30 min.

4. Conclusions

The nano-sized Nb-doped $MoSe_2$ plates are fabricated by solid-state reactions of micro-sized Mo and Se reacting with Nb at 800 □ for 2 h in an efficient reaction with inert atmosphere existed. The SEM images and XRD analysis both reveal that the existence of Nb plays an important role in refining the size of $MoSe_2$ nanoplates. The introduction of the Nb-doped $MoSe_2$ nanoplates improved the tribological properties of base oil. Moreover, the $Mo_{0.95}Nb_{0.05}Se_2$ nanoplates showed better friction reduction performance than other nanoplates did under the present experimental conditions. The differences of tribological properties are mainly ascribed to their morphology structures. The Nb-MoSe2 nanoplates with thinner and smaller morphologies could form a more stable tribofilm on the rubbing surface, as a result, the $Mo_{0.95}Nb_{0.05}Se_2$ nanoflakes present a better tribological property than other nanoplates.

Acknowledgements

This work was financially supported by National Natural Science Foundation of China (51275213) and the Jiangsu National Nature Science Foundation (BK2011534).

References

[1] W. A. Abdallah, and E. Nelson, J. Mater. Sci. **40**, 2679 (2005).
[2] V. G. Pol, S. V. Pol, and A. Gedanken, J. Nano Res. **3**, 15 (2008).
[3] H. Q. Shi, X. D. Zhou, Y. S. Lin, and X. Fu, Mater. Lett. **62**, 3649 (2008).

[4] S. V. Pol, V. G. Pol, J. M. Calderon-Moreno, and A. Gedanken, J Phys. Chem. C **112**, 5356 (2008).
[5] D. H. GALVAN, Mod. Phys. Lett. B. **18**, 35 (2004).
[6] J. M. Huang, and D. F. Kelley, Chem. Mater. **12**, 2825 (2000).
[7] F.S. Ohuchi, T. Shimada, and B.A. Parkinson, J. Cryst. Growth. **111**, 1033 (1991).
[8] A. Kumar, and P. K. Ahluwalia, Physical B. **407**, 4627 (2012).
[9] T. Polcara, M. Evaristob, and A. Cavaleiro, Wear **266**, 388 (2009).
[10] A. M. Kovalchenko, O. I. Fushchich and S.Danyluk, Wear **290**, 106 (2012).
[11] W. J. Li, L. F. Hui, M. Z. Wang, H. Tang, and C. S. Li, Cryst. Res. Technol. 47, 876 (2012).
[12] H. Tang, K. S. Cao, Q. Wu, C. S. Li, X. F. Yang, and X. H. Yan, Cryst. Res. Technol. **46**, 195 (2011)
[13] D. J. Norris, A. L. Efros, and S. C. Erwin, Science **319**, 1776 (2008).
[14] S. Y. Hu, C. H. Liang, K. K. Tiong and Y. S. Huang, J. Alloy Compd. **422**, 249 (2007).
[15] S. Y. Hu, C. H. Liang, K. K. Tiong, Y . C. Lee and Y. S. Huang, J. Cryst. Growth. **285**, 408 (2005).
[16] A. M. Vora, Chalcogenide Lett. **5**, 17 (2008).
[17] M. M. Vora and A. M. Vora, Chalcogenide Lett. **5**, 65 (2008).
[18] A. M. Vora, Cryst. Res. Technol. **42**, 286 (2007).
[19] M. M. Vora and A. M. Vora, Cryst. Res. Technol. **42**, 50 (2007).
[20] T. Joseph Sahaya Anand and S. Shariza, Electrochimica Acta. **81**, 64 (2012).